Switching performance of optically generated spin current at the graphene edge

Yuan Tian [ORCID],[1,*] M. Shoufie Ukhtary [ORCID],[1,2,†] and Riichiro Saito [ORCID][1]

[1]*Department of Physics, Tohoku University, Sendai 980-8578, Japan*
[2]*Research Center for Quantum Physics, National Research and Innovation Agency (BRIN), Tangerang Selatan 15314, Indonesia*

We investigate the response of the optically generated spin current as a function of time at the graphene edge for a possible application of optospintronic devices. The spin current is generated by optically excited edge plasmon in which the induced electric field is rotating on the graphene plane. According to the inverse Faraday effect, the in-plane rotation of electric field generates magnetization in the direction perpendicular to the graphene plane. The diffusive spin current flows by decaying distribution of the magnetization from the edge. By solving the time-dependent, diffusion equation in the presence/absence of the spin-source term, we evaluate the on/off response of spin current. The switching speed becomes fast when the spin-diffusion length is sufficiently large compared with the decaying length of the magnetization.

I. INTRODUCTION

Surface plasmons (SPs) can confine electric fields to the vicinity of a material surface due to their evanescent nature [1–5]. In particular, the attenuation of the electric field perpendicular to the surface generates a phase difference between each component of the electric field, i.e., the electric field parallel and perpendicular to the surface has a phase difference of $\pi/2$, similar to that of circularly polarized light (CPL) [6–9]. This phase difference creates a unique spin angular momentum transverse to the direction of propagation of the electromagnetic wave, in contrast to the longitudinal spin of conventional CPL [6–11]. This spin exerts a mechanical torque on the particle, causing it to rotate around its axis, which could be used for nanoscale rotators [11–14]. Furthermore, the spin of SP induces orbital motion of electrons inside the metal, which generates magnetization. This effect is known as the inverse Faraday effect [7,8,15]. In this paper, we propose a mechanism by which the inverse Faraday effect can be used to optically generate spin currents in graphene and switch currents with response rates up to 10 GHz.

Manipulation of spin current is a novel technique in the field of spintronics, which promises new designs for memory storage and logic circuits [16]. It is expected that a device using spin current instead of electric current will have a better energy efficiency, since pure spin current generates less heat than an electric current. Although methods for generating spin current such as either spin Hall effect, spin injection, or a spin valve and manipulation of magnetization by light pulse are well established, these conventional methods need either complicated structure or magnetic material [16–20], which limits the speed of the response of spintronic devices. Recently,

Oue and Matsuo showed optical generation of spin current without magnetic materials [21–23]. They showed that SP on the surface of a three-dimensional (3D) metal can generate a spin current in the direction perpendicular to the surface by utilizing the inverse Faraday effect [21–23]. In particular, the spin current can be tuned by changing the frequency of the SP. The induced spin current might be observed by using inverse Hall effect [16] or the Kerr effect measurement [24].

In a previous work, we proposed that edge plasmon in graphene ribbon generates an in-plane spin current which is convenient for making spintronic devices [25]. Edge plasmon is SP that is confined near the edge of a two-dimensional (2D) material [26–31]. Similar with SP, the spin of edge plasmon is transverse. However, the direction is out of plane [26]. The induced magnetization decays with increasing distance from the edge, which induces spin current that flows on the surface [25]. Since we can switch on/off the photoexcited magnetization by a pulse of light, it is important to evaluate how fast the spin current can be switched on/off as a function of time. Here, by adopting the time-dependent diffusion equation for the spin current, we theoretically evaluate the switching performance of these optospintronic devices.

In this paper, we consider the switching speed of the spin current generated by edge plasmon at one edge of a semi-infinite graphene as a realistic situation of a device in which the in-plane spin current flows in the direction perpendicular to the edge, which becomes simpler than our previous case of graphene ribbons [25]. In the previous work, we show that the direction of spin current by edge plasmon can be controlled by changing the gate voltage (or the Fermi energy) [25]. However, controlling the gate voltage for switching the spin current is not easy for realizing a nanoscale device. Thus, in this paper, we discuss the switching of spin current, not by the gate voltage, but by turning on and off the light that generates and removes the magnetization, respectively. We presented the evaluation of response time by considering the effects of both spin relaxation and plasmon decay lengths. We found that

*tian@flex.phys.tohoku.ac.jp
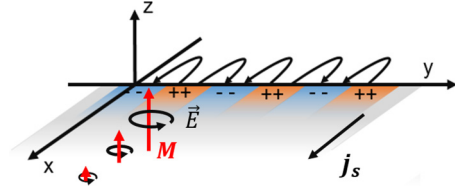†shoufie@flex.phys.tohoku.ac.jp

FIG. 1. Edge plasmon propagates along the edge of a semi-infinite graphene (xy plane and $x > 0$). The electric field on graphene ($x > 0$) decays spatially from the edge. Since the electric field in the x direction has a $\pi/2$ phase difference from the phase in the y direction, electric field is rotating on the graphene plane as a function of time, which generates spatially decaying magnetization M. The decaying magnetization induces surface spin current j_s that flows in the direction perpendicular to the edge.

the spin current can be switched with response speed up to 10 GHz.

Organization of the paper is as follows. In Sec. II, we explain how to obtain the spin current at the edge of graphene. In Sec. III, we show the calculated results of the spin current as a function of position and time. We then determine the switching speed by removing the edge plasmon. In Sec. IV, we discuss the results and in Sec. V, the summary of the paper is given.

II. METHOD

In this section, we first discuss how to obtain the electric field of the edge plasmon at the edge of graphene. We then show that the electric field is rotating as a function of time on the plane of graphene, which generates spatially decaying magnetization from the edge according to the inverse Faraday effect. Finally, we derive the spin current by solving the time-dependent spin-diffusion equations, in which the induced magnetization appears as a source term.

A. Electric field of edge plasmon

We consider an edge plasmon that propagates in the y direction at one edge ($x = 0$) of a semi-infinite graphene in the xy plane as shown in Fig. 1. The electric field on the surface of graphene is defined by

$$\boldsymbol{E}(x, y, t) = -\nabla \Phi(x, y, t) - \partial_t \boldsymbol{A}(x, y, t), \quad (1)$$

where $\Phi(x, y, t)$ and $\boldsymbol{A}(x, y, t)$ are the scalar and vector potentials on the surface of graphene, respectively. The propagating $\Phi(x, y, t)$ and $\boldsymbol{A}(x, y, t)$ are expressed by $\Phi(x, y, t) = \Phi_q(x)e^{i(qy-\omega t)}$ and $\boldsymbol{A}(x, y, t) = \boldsymbol{A}_q(x)e^{i(qy-\omega t)}$, with expressions of $\Phi_q(x)$ and $\boldsymbol{A}_q(x)$ satisfying the following differential equations [25]:

$$\left(\partial_x^2 - 2\kappa^2\right)\Phi_q(x) = \frac{e\kappa}{\epsilon_0} n_q(x), \quad (2)$$

$$\left(\partial_x^2 - 2\kappa^2\right)A_{qx}(x) = -\mu_0 \kappa J_{qx}(x), \quad (3)$$

$$\left(\partial_x^2 - 2\kappa^2\right)A_{qy}(x) = -\mu_0 \kappa J_{qy}(x), \quad (4)$$

where A_{qx} and A_{qy} is the x and y component of $\boldsymbol{A}(x)$, respectively, e is the elementary charge, and ϵ_0 and μ_0 represent vacuum permittivity and permeability. Here, κ is the decay

constant of electric field in the z direction and is defined as $\kappa = \sqrt{q^2 - \omega^2/c^2}$ [7].

By solving Eqs. (1)–(4) we get the expression of the electric field of the edge plasmon as follows [25,26]:

$$E_x(x, y, t) = -\gamma \left[\frac{i\omega\mu_0\sigma(\omega)\kappa}{\gamma^2 - \xi_q^2} - 1\right]\phi_0 e^{-\gamma x + i(qy-\omega t)}, \quad (5)$$

$$E_y(x, y, t) = iq \left[\frac{i\omega\mu_0\sigma(\omega)\kappa}{\gamma^2 - \xi_q^2} - 1\right]\phi_0 e^{-\gamma x + i(qy-\omega t)}, \quad (6)$$

where we define the retarded wave vector ξ_q^2,

$$\xi_q^2 = 2\kappa^2 - i\omega\mu_0\sigma(\omega)\kappa, \quad (7)$$

and decay constant γ,

$$\gamma(\omega, q) = \sqrt{2}\kappa \sqrt{\frac{1 + \frac{i\sigma(\omega)\kappa}{2\epsilon_0\omega}}{1 + \frac{i\sigma(\omega)\kappa}{\epsilon_0\omega}}}. \quad (8)$$

$\sigma(\omega)$ here represents the Drude conductivity as follows [32]:

$$\sigma(\omega) = \frac{ie^2 E_F}{\pi \hbar(\hbar\omega + i\Gamma)}, \quad (9)$$

where E_F and Γ denote, respectively, the Fermi energy of graphene and the scattering rate of the electron. In this work, we take $E_F = 0.05$ eV and $\Gamma = 0.1$ meV [25].

$E_x(x, y, t)$ and $E_y(x, y, t)$ denote the x and y components of the electric field, respectively. It is noted that the $E_x(x, y, t)$ and $E_y(x, y, t)$ have a phase difference of $\pi/2$, similar to the CPL. Therefore, the electric field of edge plasmon at each point rotates as a function of time, which corresponds to the nonzero spin angular momentum of light [6,7]. It is noted that in the case of CPL, the spin angular momentum is longitudinal to the propagation direction, while in the case of edge plasmon, the spin angular momentum is transverse and out of plane [25,26]. The nonzero spin angular momentum of light on the surface of graphene generates a finite magnetization, which will be discussed in Sec. II B.

Frequency of the edge plasmon is obtained by solving the boundary conditions at $x = 0$ [26,27]. It is noted that in the case of the nonretardation region, $\kappa \approx q$, the frequency of edge plasmon is analytically given by

$$\omega(q) = \sqrt{\frac{2}{3}} \sqrt{\frac{e^2 E_F q}{2\pi \epsilon_0 \hbar^2}} \equiv \sqrt{\frac{2}{3}} \omega_{SP}(q), \quad (10)$$

where $\omega_{SP}(q)$ is the frequency of the surface plasmon in graphene [1,27,33]. Thus, the frequency of edge plasmon is smaller than that of surface plasmon by the factor $\sqrt{2/3}$.

B. Spin-diffusion equation

Light with spin angular momentum can induce a magnetization in a metal, which is referred to as the inverse Faraday effect [7,15,34]. The induced magnetization $\boldsymbol{M}_{ind}$ is expressed by [15]

$$\boldsymbol{M}_{ind} = -i \frac{|\sigma(\omega)|^2}{4\omega e\bar{n}}(\boldsymbol{E}^* \times \boldsymbol{E}), \quad (11)$$

where $\bar{n}$ is the charge density at the thermal equilibrium. In the case of graphene, $\bar{n}$ is given by $\bar{n} = [E_F/(\sqrt{\pi}\hbar v_F)]^2$ [1]. It is

noted that the spin angular momentum of light is proportional to the product of $(\boldsymbol{E}^* \times \boldsymbol{E})$, which is not zero only if there is a phase difference between the x and y components of $\boldsymbol{E}$ [6,7].

Substituting Eqs. (5) and (6) into Eq. (11), the magnetization induced by edge plasmon on the graphene is expressed as follows:

$$\boldsymbol{M}_{\text{ind}}(x) = -\hat{z}\frac{|\sigma(\omega)|^2\gamma}{\omega e \bar{n} q}\left|\frac{i\omega\mu_0\sigma(\omega)\kappa}{\gamma^2 - L_q^2} - 1\right|^2 E_0^2 e^{-2\gamma x}, \quad (12)$$

where we define $E_0 = q\phi_0$. From Eq. (12), we understand that the edge plasmon induces a magnetization pointing in the direction perpendicular to the surface of graphene ($\hat{z}$). The induced magnetization is constant in time but exponentially decaying ($e^{-2\gamma x}$) measured from the edge of graphene. Thus, the edge plasmon induces spatially decaying magnetization on graphene surface. A similar magnetization is also induced in the case of surface plasmon in 3D metals [21–23]; however, the magnetization is distributed inhomogeneously in the perpendicular direction to the surface.

The magnetization that is induced by edge plasmon polarizes the spin of individual electrons and generates spin accumulation, which is described by the spin-diffusion equation as a source term, as follows [21–23,25]:

$$\left(\nabla^2 - \frac{1}{\lambda^2} - \frac{\partial}{\partial t}\frac{t_{\text{sf}}}{\lambda^2}\right)\delta\mu(x,t) = 8\mu_{\text{B}}\mu_0\gamma^2\frac{\boldsymbol{M}_{\text{ind}}(x)}{d}, \quad (13)$$

where $\delta\mu(x,t)$ is defined by the shift of chemical potential by the spin accumulation in units of eV. t_{sf} and λ are the spin relaxation time and spin-diffusion length, respectively [16], d denotes the thickness of graphene, and we adapt $d \approx 1$ Å. The $\delta\mu(x,t)$ is solved with the Neumann boundary condition, which is $\partial_x\delta\mu = 0$ at $x = 0$, by using the finite difference time domain (FDTD) method and analytically [see Eq. (22)]. Since the induced magnetization is spatially decaying from the edge of graphene, we then expect that the $\delta\mu(x,t)$ is decaying not only as a function of time, but also as a function of x. The obtained $\delta\mu(x,t)$ generates diffusive spin current, which is expressed as follows [16,19]:

$$\boldsymbol{J}_s(x,t) = \frac{\sigma_0}{2e}\nabla\delta\mu(x,t). \quad (14)$$

Here, σ_0 is the DC conductivity of graphene, that is obtained by substituting $\omega = 0$ in Eq. (9). We use DC conductivity to describe the spin current because the spin current is driven by the spatially decaying magnetization which is not a function of time, as is given in Eq. (12). Since the magnetization is a function of x, then the $\boldsymbol{J}_s(x,t)$ flows on the surface of graphene in the x direction, too. Since spin generation by edge plasmon is our idea, we do not know of any results similar to this study in the literature. One might consider it similar to the paper by Oue and Matsuo [21]. However, we would like to point out that their spin generation is not due to the edge plasmon in 2D materials, but rather to the surface plasmon on 3D metal surfaces. Furthermore, the direction of the spin current in Oue and Matsuo is perpendicular to the surface, whereas the direction of the spin current in this study is in plane. Thus, they are not similar, and the in-plane spin current is considered to be more useful.
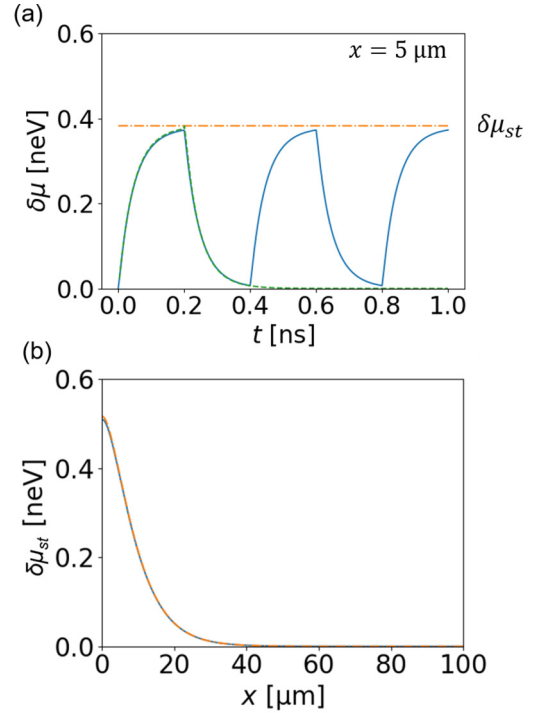

FIG. 2. Spin accumulation $\delta\mu$ (a) given as a function of time, at $x = 5$ μm, under a source term of light that is turned on (0.2 ns) and off (0.2 ns) with a period of 0.4 ns. The blue solid line represents the result obtained from the FDTD method, while the green dashed line represents the analytical expression of $\delta\mu$ given in Eqs. (21) and (22). It is observed that the $\delta\mu$ reaches the steady state (orange dashed-dotted line) within 0.2 ns. Further, when the source term is turned off, $\delta\mu$ vanishes within 0.2 ns. This means $\delta\mu$ can respond to the source term with frequency up to 10 GHz. The orange dashed line represents the $\delta\mu_{\text{st}}(x = 5 \mu\text{m})$ as given in Eq. (15). (b) $\delta\mu_{\text{st}}(x)$ as a function of distance from the edge x. $\delta\mu_{\text{st}}(x)$ is confined to the edge with decay length of less than 40 μm. The blue solid line represents the result obtained by FDTD, while the orange dashed line represents the $\delta\mu_{\text{st}}$ given in Eq. (15). Here we adopt $\omega = 4.32$ THz, $E_0 = 860$ V/m, $\lambda = 6.344$ μm, $\gamma = 0.13$ μm^{-1}, and $t_{\text{sf}} = 58.5$ ps.

III. RESULTS

First, we show the numerically calculated result of the $\delta\mu(x,t)$, which are obtained by solving Eqs. (13) and (14) by FDTD calculation. To investigate how fast the $\delta\mu$ responds to an external source, we apply a periodic light source term which turns on (0.2 ns) and off (0.2 ns) in a period of 0.4 ns. We obtain $\delta\mu$ as a function of t for a given $x = 5$ μm, which is plotted in Fig. 2(a). Here we adopt $\omega = 4.32$ THz, $E_0 = 860$ V/m, $\gamma = 0.13$ μm^{-1}, $\lambda = 6.344$ μm, and $t_{\text{sf}} = 58.5$ ps. The values of $\omega = 4.32$ THz and $\lambda = 6.344$ μm correspond to the case that the diffusion length becomes comparable to the decay length of magnetization, $\lambda = 1/2\gamma(\omega)$. With this value of ω and λ, we can observe the crossover phenomena between the spin-diffusion regime [$\lambda \gg (1/2\gamma)$] and the decaying dominant region [$\lambda \ll (1/2\gamma)$]. We took the value of $\lambda = 6.344$ μm and $t_{\text{sf}} = 58.5$ ps from the measurement conducted by Raes *et al.* [35]. The value of 860 V/m corresponds to the laser intensity of 100 mW/cm^2. It is observed that the $\delta\mu(x,t)$ saturates around 0.5 neV within 0.2 ns, which we

call the steady state denoted by $\delta\mu_{\text{st}}(x)$. After turning off the source term, $\delta\mu(x, t)$ vanishes in less than 0.2 ns. This means that with the given parameters, $\delta\mu(x, t)$ can respond to the source term with frequency up to 10 GHz.

We further investigate the solution of $\delta\mu_{\text{st}}(x)$, which corresponds to the case of $\partial\delta\mu(x, t)/\partial t = 0$ in Eq. (13). The $\delta\mu_{\text{st}}(x)$ is expressed as follows:

$$\delta\mu_{\text{st}}(x) = A \exp\left(-2\gamma x\right) + B \exp\left(-\frac{x}{\lambda}\right), \quad (15)$$

where A and B are coefficients for describing the contribution of the induced magnetization and the spin diffusion to $\delta\mu$, respectively. The coefficient A is obtained by substituting Eq. (15) into Eq. (13), which is given as follows:

$$A = \frac{2\mu_B\mu_0}{d} \frac{(2\gamma\lambda)^2}{(2\gamma\lambda)^2 - 1} M_{\text{ind}}(0). \quad (16)$$

On the other hand, the coefficient B is determined from the Neumann boundary condition: $\partial_x\delta\mu_{\text{st}}(x) = 0$ at $x = 0$, from which we get $B = -2\gamma\lambda A$.

In Fig. 2(b), the $\delta\mu_{\text{st}}(x)$ [Eq. (15)] is plotted by an orange dash-dotted line as a function of x together with the result obtained by FDTD (blue solid line), whose agreement is satisfactory. It is observed that $\delta\mu_{\text{st}}(x)$ is confined to the edge, which is expressed by a linear combination of exponentially decaying functions. The maximum $\delta\mu_{\text{st}}(x)$ occurs at the edge, which reaches up to 0.5 neV. Furthermore, the decay length of $\delta\mu_{\text{st}}(x)$ is about 20 μm.

When $x = 0$, Eq. (15) determines the largest possible value of $\delta\mu$ for given λ and γ. In Fig. 3(a), we plot Eq. (15) for $x = 0$ as a function of λ and γ, from which we find that the $\delta\mu_{\text{st}}$ increases with increasing λ and decreasing γ. In Fig. 3(b) we plot $\delta\mu_{\text{st}}$ [Eq. (15)] as a function of λ at $x = 0$ for several values of γ. When $\lambda = 300$ μm, $\gamma = 0.12$ μm^{-1}, maximum $\delta\mu$ reaches 100 neV. From the calculation, we can suggest to fabricate graphene with a larger spin-diffusion length λ and then we excite edge plasmon with small decay constant γ (i.e., a longer decay length) in order to obtain larger spin accumulation. It is noted that γ depends on ω and q as is expressed in Eq. (8). Small γ can be obtained by decreasing the frequency of edge plasmon, which is described in detail in our earlier work [25].

In Fig. 3(c), we plot spin current density J_s in units of μA/m as a fucntion of x for several values of λ from 1 to 5 μm. Here, spin current density J_s is calculated by substituting Eq. (15) into Eq. (14). As seen in Fig. 3(c), J_s increases with increasing λ The value J_s might be observed experimentally if the length of the edge is larger than 1 mm.

To further identify the time-dependent behavior of $\delta\mu(x, t)$, we have obtained the analytical solution of $\delta\mu(x, t)$ by the Green's function method. The Green's function of the diffusion equation given in Eq. (13) is expressed as follows:

$$G(x, t, x', t') = -\exp\left(-\frac{t - t'}{t_{\text{sf}}}\right) \frac{\Theta(t - t')\Theta(t')\lambda}{\sqrt{4\pi t_{\text{sf}}(t - t')}}$$
$$\times \left\{\exp\left[-(x - x')^2 k_a^2\right]\right.$$
$$\left.+ \exp\left[-(x + x')^2 k_a^2\right]\right\}, \quad (17)$$
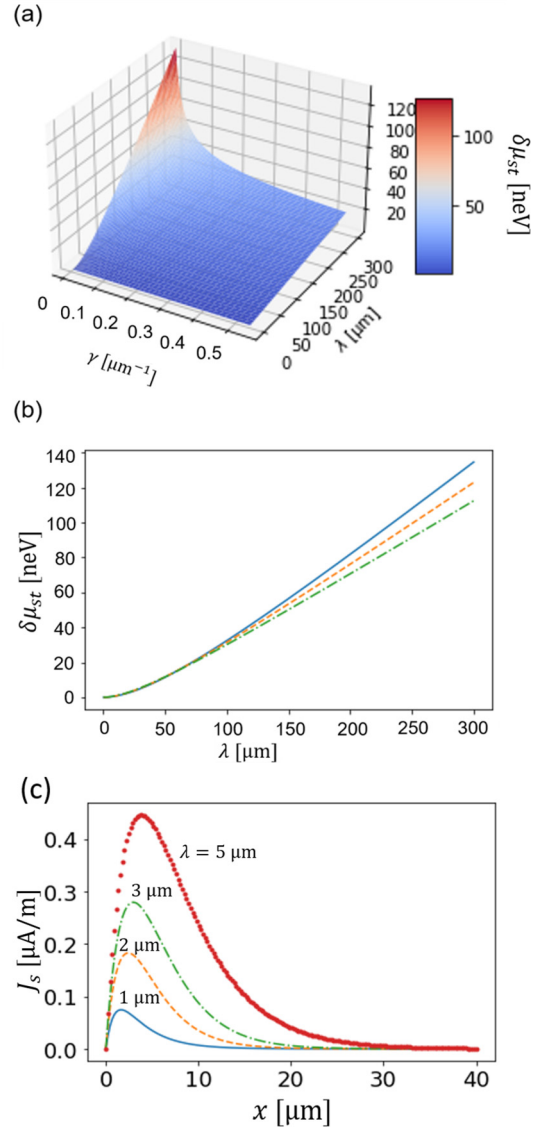

(a)

(b)

(c)

FIG. 3. Maximum spin accumulation $\delta\mu_{\text{st}}$ at $x = 0$ (a) given as a function of spin-diffusion length λ and edge plasmon decay constant γ. Larger λ and smaller γ give a larger maximum $\delta\mu_{\text{st}}$. (b) $\delta\mu_{\text{st}}$ as a function of λ, for several values of γ: $\gamma = 0.070$ μm^{-1} for the blue solid line, $\gamma = 0.094$ μm^{-1} for the orange dashed line, and $\gamma = 0.12$ μm^{-1} for the green dash-dotted line. We find that $\delta\mu_{\text{st}}$ reaches up to 140 neV when $\lambda = 300$ μm and $\gamma = 0.070$ μm^{-1}. Here we adopt $E_0 = 860$ V/m and $t_{\text{sf}} = 58.5$ ps. (c) Spin current density [Eq. (14)] as a function of x for several values of λ. Peak spin current appears from a distance from the edge. This distance and the peak spin current value increases with increasing λ. Here we adopt $\omega = 4.32$ THz, $E_0 = 860$ V/m, $\gamma = 0.13$ μm^{-1}, and $t_{\text{sf}} = 58.5$ ps.

where $\Theta(x)$ represents the Heaviside function. k_a is the time-dependent diffusion parameter, which is written as follows:

$$k_a = \sqrt{\frac{t_{\text{sf}}}{4(t - t')\lambda^2}}. \quad (18)$$

It is noted that the Green's function given in Eq. (17) satisfies the Neumann boundary condition. When the source term is turned on and spin is accumulating, the $\delta\mu(x, t)$ can then be

obtained as follows:

$$\delta\mu(x,t) = \frac{8\mu_0\mu_B\gamma^2}{d} \int_{-\infty}^{\infty} dt' \int_{0}^{\infty} dx' \, G(x,t,x',t') M_{ind}(x').$$
(19)

On the other hand, when the source term is turned off, the $\delta\mu(x,t)$ starts to relax and decays away from the steady state. Thus, the $\delta\mu(x,t)$ is written as follows:

$$\delta\mu(x,t) = \frac{t_{sf}}{\lambda^2} \int_{0}^{\infty} dx' G(x,t,x',0) \, \delta\mu_{st}(x'),$$
(20)

where $\delta\mu_{st}(x)$ expressed in Eq. (15) corresponds to the fully accumulated condition when the source is turned on after a sufficiently long time. By substituting Eq. (17) into Eqs. (19) and (20), and by noting that the expression includes a Gaussian integral, we can further obtain the analytical expression of $\delta\mu$ given in terms of the Gauss error function as follows:

$$\delta\mu(x,t) = \frac{8\mu_0\mu_B\gamma^2}{d} M_{ind}(0) \int_{0}^{t} dt' e^{(4\lambda^2\gamma^2-1)(t-t')/t_{sf}}$$
$$\times \left[e^{-2\gamma x}\mathrm{erfc}\left(\frac{\gamma - k_a^2 x}{k_a}\right) + e^{2\gamma x}\mathrm{erfc}\left(\frac{\gamma + k_a^2 x}{k_a}\right) \right],$$
(21)

for the accumulation of $\delta\mu$ and

$$\delta\mu(x,t) = A e^{(4\lambda^2\gamma^2-1)(t/t_{sf})}$$
$$\times \left[e^{-2\gamma x}\mathrm{erfc}\left(\frac{\gamma - k_a^2 x}{k_a}\right) + e^{2\gamma x}\mathrm{erfc}\left(\frac{\gamma + k_a^2 x}{k_a}\right) \right]$$
$$+ B\left[e^{-x/\lambda}\mathrm{erfc}\left(\frac{\frac{1}{2\lambda} - k_a^2 x}{k_a}\right) \right.$$
$$\left. + e^{x/\lambda}\mathrm{erfc}\left(\frac{\frac{1}{2\lambda} + k_a^2 x}{k_r}\right) \right],$$
(22)

for the relaxing of $\delta\mu$. In Eqs. (21) and (22), erfc(z) represents the complementary error function of z as follows:

$$\mathrm{erfc}(z) = 1 - \frac{2}{\sqrt{\pi}} \int_{0}^{z} e^{-t^2} dt.$$
(23)

The solution obtained by the Green's function is shown by the green dashed line in Fig. 2(a). The analytical expression reproduces the FDTD results. Equation (17) implies that the switching speed of $\delta\mu(x,t)$ depends on t_{sf}, λ, γ, and position x. In the next section, we discuss the dependence of the response time on t_{sf}, λ, γ, and x.

IV. DISCUSSION

For optimizing the response speed of the present spintronic device, information concerning the response speed of spin accumulation in relation to external perturbation is important. Noticing that the shape of the $\delta\mu(x,t)$ from Fig. 2(a) can be roughly fitted with an exponential function, in Fig. 4, we fit the following exponential function to the time-dependent plot of $\delta\mu(t)$:

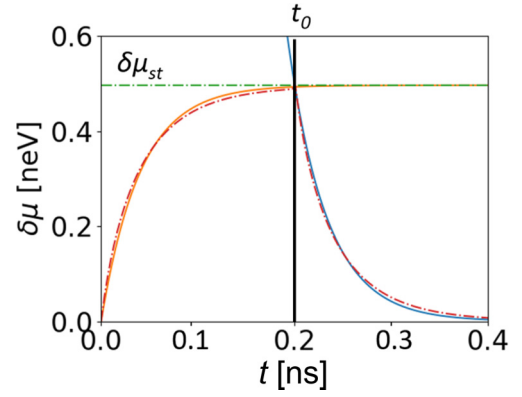$$\delta\mu(x,t) = \delta\mu_{st}(x)\left\{ 1 - \exp\left(-\frac{t}{t_a}\right) \right\},$$
(24)

FIG. 4. $\delta\mu$ as a function of time. The red dot-dashed line represents the $\delta\mu$ given in Eqs. (19) and (20). The solid orange line and solid blue line represent the fitting function of Eqs. (24) and (25), respectively. The green dash-dotted horizontal line represents $\delta\mu_{st}$, and the vertical black line denotes the $t = t_0$ in Eq. (25). Here we adopt $\omega = 4.32$ THz, $E_0 = 860$ V/m, $\gamma = 0.13\ \mu m^{-1}$, $\lambda = 6.344\ \mu m$, $x = 5\ \mu m$, and $t_{sf} = 58.5$ ps.

for the accumulation of $\delta\mu(x,t)$ and

$$\delta\mu(x,t) = \delta\mu_{st}(x)\exp\left(-\frac{t-t_0}{t_d}\right),$$
(25)

for the relaxation of $\delta\mu(x,t)$. Here, t_a and t_d are the response times for the accumulation and relaxation of $\delta\mu(x,t)$. In Fig. 4, we plot the fitted $\delta\mu(x,t)$, which is not perfect but sufficient for discussing the response times (t_a and t_d). As shown in the end of Sec. III, we will discuss how the response times depend on t_{sf}, λ, x, and γ. The response time is defined mathematically as the time necessary to reach the following $\delta\mu(x,t)$ for the accumulation $\delta\mu(x,t)$,

$$\delta\mu(x,t_a) = \left(1 - \frac{1}{e}\right)\delta\mu_{st}(x),$$
(26)

or the time it takes to decay to the following $\delta\mu(x,t)$ for the decaying $\delta\mu(x,t)$,

$$\delta\mu(x,t_d) = \frac{1}{e}\delta\mu_{st}(x),$$
(27)

where e is natural exponential number. As we see from Eq. (13), t can be scaled by t_{sf}. We define dimensionless response time $a_{a(d)}$ by

$$t_{a(d)}(t_{sf}, \lambda, x, \gamma) = a_{a(d)}(\lambda, x, \gamma) t_{sf},$$
(28)

where $a_{a(d)}(\lambda, x, \gamma)$ denotes a factor on t_{sf} whose value depends only on λ, x, and γ. We confirm by numerical calculation that $a_{a(d)}$ does not depend on t_{sf}. When $a_{a(d)}(\lambda, x, \gamma)$ is small, the response time becomes fast.

In Figs. 5(a) and 5(b), we plot $a_{a(d)}$ as a function of x and λ for the accumulation and relaxation parts, respectively. The x and λ dependence of $a_{a(d)}$ shows similar behavior. The values of a_a and a_d are almost the same; then we refer to them simply as $a(\lambda, x, \gamma)$. For a fixed value of λ, $x = 0$ always gives a small value of $a(\lambda, x, \gamma)$, which corresponds to a fast response. The value of $a(\lambda, x, \gamma)$ becomes small for a large λ for any value of x. As seen in Figs. 5(a) and 5(b), we can see that $a(\lambda, x, \gamma)$ has a local maximum for x not near the
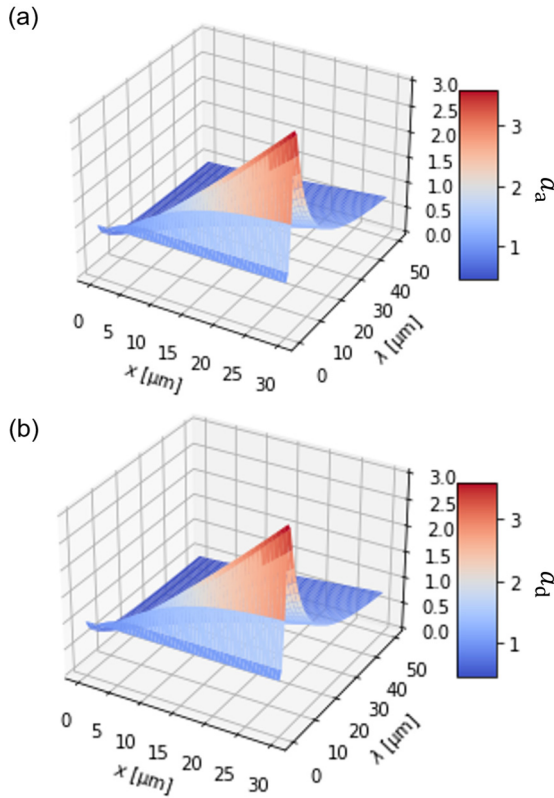
(a)

(b)

FIG. 5. Dimensionless response time $a_{\mathrm{a(d)}}(\lambda, x, \gamma) = t_{\mathrm{a(d)}}/t_{\mathrm{sf}}$ for (a) the accumulation part of $\delta\mu$ and (b) the relaxation part of $\delta\mu$. A local peak of $a_{\mathrm{a(d)}}(\lambda, x, \gamma)$ appears where $\lambda = 1/(2\gamma)$, which corresponds to a slowest response time. When $\lambda > 1/(2\gamma)$, the value of $a_{\mathrm{a(d)}}(\lambda, x, \gamma)$ becomes small for a large λ for any values of x. Here we adopt $\omega = 4.95$ THz, $E_0 = 860$ V/m, and $\gamma = 0.17$ $\mu\mathrm{m}^{-1}$.

edge. The condition for obtaining the maximum is $\lambda = 1/2\gamma$, which can be numerically checked. Thus, we conclude that the response time can be short when the spin-diffusion length (λ) is sufficiently large compared with the decay length of the

magnetization $(1/2\gamma)$. For a fixed value of λ, the response time becomes shorter with increasing γ, which corresponds to the increasing frequency of the edge plasmon (ω). However, even though the response time is shorter, as shown in Fig. 3(a), if we increase the γ, the value of $\delta\mu_{\mathrm{st}}$ decreases. Thus, we need to find the appropriate γ or ω that gives a fast response time and sufficient $\delta\mu$ to be measurable. Let us use $\lambda = 2.96$ μm for graphene, thus the $a(\lambda, \gamma)$ is maximum when $\gamma = 0.169$ $\mu\mathrm{m}^{-1}$, which corresponds to frequency of the edge plasmon $\omega = 4.59$ THz for $E_{\mathrm{F}} = 0.05$ eV. To achieve a faster response time, we can select the $\gamma = 2 \times 1/2\lambda$, so that the $\delta\mu$ does not become too small to be measurable. In this case, the frequency of the edge plasmon is around $\omega = 7.32$ THz. The corresponding response time t_a and t_d = 70.2 ps at $x = 5$ μm, which means a theoretical response frequency of 7.12 GHz. Thus we get a gigahertz response for this spintronic device.

V. CONCLUSION

In conclusion, by using the finite-difference time-domain method and the Green's function method, we investigate the response time of the spin current induced by edge plasmon at the graphene edge. The response speed is estimated to be up to 10 GHz. The condition that we obtain a faster response is that the spin-diffusion length is sufficiently large compared with the decay length of the magnetization. We suggest selecting a frequency that gives the decay length of the magnetization whose value is half of the spin-diffusion length to achieve a sufficiently fast response time with sufficient spin accumulation.

[1] M. Jablan, H. Buljan, and M. Soljačić, Phys. Rev. B **80**, 245435 (2009).

[2] M. Jablan, M. Soljačić, and H. Buljan, Proc. IEEE **101**, 1689 (2013).

[3] S. A. Maier, *Plasmonics: Fundamentals and Applications* (Springer, New York, 2007), Vol. 1.

[4] F. H. Koppens, D. E. Chang, and F. J. Garcia de Abajo, Nano Lett. **11**, 3370 (2011).

[5] Q. Bao and K. P. Loh, ACS Nano **6**, 3677 (2012).

[6] K. Y. Bliokh and F. Nori, Phys. Rep. **592**, 1 (2015).

[7] K. Y. Bliokh, A. Y. Bekshaev, and F. Nori, Phys. Rev. Lett. **119**, 073901 (2017).

[8] K. Y. Bliokh, A. Y. Bekshaev, and F. Nori, New J. Phys. **19**, 123014 (2017).

[9] F. Kalhor, T. Thundat, and Z. Jacob, Appl. Phys. Lett. **108**, 061102 (2016).

[10] A. Aiello, P. Banzer, M. Neugebauer, and G. Leuchs, Nat. Photonics **9**, 789 (2015).

[11] K. Y. Bliokh, A. Y. Bekshaev, and F. Nori, Nat. Commun. **5**, 3300 (2014).

[12] A. Canaguier-Durand and C. Genet, Phys. Rev. A **89**, 033841 (2014).

[13] A. Canaguier-Durand, A. Cuche, C. Genet, and T. W. Ebbesen, Phys. Rev. A **88**, 033831 (2013).

[14] H. Chen, W. Lu, X. Yu, C. Xue, S. Liu, and Z. Lin, Opt. Express **25**, 32867 (2017).

[15] R. Hertel, J. Magn. Magn. Mater. **303**, L1 (2006).

[16] S. Maekawa, S. O. Valenzuela, T. Kimura, and E. Saitoh, *Spin Current* (Oxford University Press, New York, 2017).

[17] G. L. da Silva, L. H. Vilela-Leo, S. M. Rezende, and A. Azevedo, J. Appl. Phys. **111**, 07C513 (2012).

[18] S. Takahashi and S. Maekawa, Sci. Technol. Adv. Mater. **9**, 014105 (2008).

[19] S. Takahashi and S. Maekawa, J. Phys. Soc. Jpn. **77**, 031009 (2008).

[20] S. Iihama, Q. Remy, J. Igarashi, G. Malinowski, M. Hehn, and S. Mangin, J. Phys. Soc. Jpn. **90**, 081009 (2021).

[21] D. Oue and M. Matsuo, Phys. Rev. B **101**, 161404(R) (2020).

[22] D. Oue and M. Matsuo, Phys. Rev. B **102**, 125431 (2020).

[23] D. Oue and M. Matsuo, New J. Phys. **22**, 033040 (2020).

[24] A. Hernández-Mínguez, K. Biermann, S. Lazić, R. Hey, and P. V. Santos, Appl. Phys. Lett. **97**, 242110 (2010).

[25] M. S. Ukhtary, Y. Tian, and R. Saito, Phys. Rev. B **103**, 245428 (2021).

[26] M. S. Ukhtary, M. Maruoka, and R. Saito, Phys. Rev. B **100**, 155432 (2019).

[27] J. C. Song and M. S. Rudner, Proc. Natl. Acad. Sci. USA **113**, 4658 (2016).

[28] A. L. Fetter, Phys. Rev. B **32**, 7676 (1985).

[29] A. Y. Nikitin, F. Guinea, F. J. García-Vidal, and L. Martín-Moreno, Phys. Rev. B **84**, 161407(R) (2011).

[30] W. Wang, P. Apell, and J. Kinaret, Phys. Rev. B **84**, 085423 (2011).

[31] W. Wang and J. M. Kinaret, Phys. Rev. B **87**, 195424 (2013).

[32] Y. Harada, M. S. Ukhtary, M. Wang, S. K. Srinivasan, E. H. Hasdeo, A. R. T. Nugraha, G. T. Noe, Y. Sakai, R. Vajtai, P. M. Ajayan, R. Saito, and J. Kono, ACS Photonics **4**, 121 (2017).

[33] M. S. Ukhtary and R. Saito, Carbon **167**, 455 (2020).

[34] H.-L. Zhang, Y.-Z. Wang, and X.-J. Chen, J. Magn. Magn. Mater. **321**, L73 (2009).

[35] B. Raes, J. E. Scheerder, M. V. Costache, F. Bonell, J. F. Sierra, J. Cuppens, J. Van de Vondel, and S. O. Valenzuela, Nat. Commun. **7**, 11444 (2016).